



Coulomb blockade in suspended Si₃N₄ -coated single-walled carbon nanotubes

Citation

Peng, H. B., and J. A. Golovchenko. 2004. Coulomb Blockade in Suspended Si₃N₄ - Coated Single-Walled Carbon Nanotubes. Applied Physics Letters 84, no. 26: 5428. doi:10.1063/1.1765733.

Published Version

doi:10.1063/1.1765733

Permanent link

<http://nrs.harvard.edu/urn-3:HUL.InstRepos:29405820>

Terms of Use

This article was downloaded from Harvard University's DASH repository, and is made available under the terms and conditions applicable to Other Posted Material, as set forth at <http://nrs.harvard.edu/urn-3:HUL.InstRepos:dash.current.terms-of-use#LAA>

Share Your Story

The Harvard community has made this article openly available. Please share how this access benefits you. [Submit a story](#).

[Accessibility](#)

Coulomb blockade in suspended Si_3N_4 -coated single-walled carbon nanotubes

H. B. Peng and J. A. Golovchenko^{a)}

Division of Engineering and Applied Sciences, Harvard University, Cambridge, Massachusetts 02138

(Received 14 January 2004; accepted 30 April 2004; published online 17 June 2004)

Uniform coaxial coating of suspended single-walled carbon nanotubes with high-quality dielectric silicon nitride has been obtained by low-pressure chemical vapor deposition. A three-terminal device has been demonstrated by coating a suspended metallic nanotube grown directly on contacting metal electrodes with subsequent patterning of a top gate electrode. Large charging energies have been observed in the suspended nanotubes and the conversion factor from gate voltage to the electrostatic potential in the nanotube approaches unity, which can be attributed to the device geometry. © 2004 American Institute of Physics. [DOI: 10.1063/1.1765733]

Coating carbon nanotubes¹ is of great interest because it provides a way to obtain nanowires of different materials,^{2–4} and also because the physical properties of exposed nanotubes are sensitive to the surrounding environment^{5,6} making it important to passivate nanotubes with coatings in practical devices.^{7–9} Interesting phenomena have been observed in superconducting metal nanowires prepared by using carbon nanotubes as templates.^{3,4} The coating behavior of a variety of metals on suspended single-walled nanotubes (SWNTs) has also been investigated.² Coating nanotubes with dielectric materials is crucial in making electronic devices and recently there have been reports on coating nanotubes dispersed in solutions with oxides by chemical reactions.^{10–12} Here we describe coating individual suspended and electrically contacted SWNTs with dielectric materials and address their electronic properties thereafter.

Previously¹³ we showed that vacuum-deposited Fe serves as a reliable and convenient catalyst to direct the methane chemical vapor deposition (CVD) growth of SWNTs on specific sites and to successfully grow electrically contacted SWNTs directly on metals electrodes. In this letter it is shown that as-grown individual suspended SWNTs can be coated uniformly with high-quality silicon nitride by low-pressure chemical vapor deposition (LPCVD). Furthermore, we demonstrate a three-terminal device by coaxially coating a suspended metallic SWNT with a nitride insulator and a metal gate electrode, and investigate the Coulomb blockade phenomenon at low temperatures.

In our experiments, a pair of several micron wide metal electrodes (Pt 50 nm/Cr 50 nm) with Fe catalyst on top, spaced apart end on with a gap between them, were patterned in the center of self-supporting 0.5- μm -thick Si_3N_4 membranes by optical lithography and lift off processing.¹³ [Fabrication on self-supporting nitride films makes viewing devices with a transmission electron microscope (TEM) practical.] The Fe catalyst evaporation is typically between 8 and 16 Å, as monitored by a quartz crystal oscillator in the evaporation chamber. A focused ion beam (FIB) was used to mill the gap area between the electrodes all the way through the Si_3N_4 membranes. Figure 1(a) illustrates a cross-sectional view of the device structure. Afterwards, CVD

nanotube growth was carried out in a methane flow of 200 sccm at 900 °C for less than 5 min at atmospheric pressure, which usually yields one or a few suspended SWNTs bridging the two electrodes. Under the above mentioned growth condition, the as-grown SWNTs are high quality with little amorphous carbon, as observed by TEM. Subsequent coating of those as-grown suspended SWNTs with silicon nitride was done by LPCVD at 720 °C in a mixed flow of SiH_2Cl_2 (100 sccm) and NH_3 (140 sccm) at a pressure ~ 1 Torr, with a nitride growth rate on planar substrates approximately 2.5 nm per min reaction time. The index of refraction for the deposited silicon nitride is 2.00 ± 0.05 as measured by an ellipsometers, which indicates a stoichiometric nitride Si_3N_4 .

Figure 1(b) shows a scanning electron microscope (SEM) image of as-grown suspended SWNTs bridging electrodes over a gap $\sim 2.4 \mu\text{m}$ wide. The CVD growth time for this sample is 1.5 min in a methane flow (200 sccm) at 900 °C. As seen in the image, only two nanotubes are crossing the gap, with one nanotube barely visible at the upper edge of the electrodes. After LPCVD at 720 °C in a mixed flow of SiH_2Cl_2 (100 sccm) and NH_3 (140 sccm) for 40 min

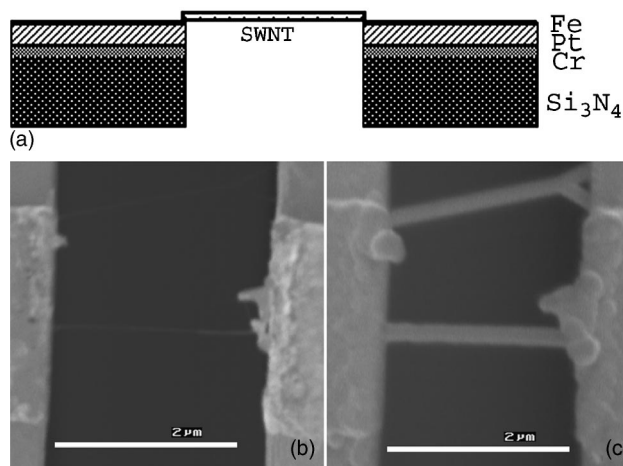


FIG. 1. (a) Schematic cross section of devices with suspended SWNTs grown directly on metal electrodes across a gap ion milled all the way through a self-supporting Si_3N_4 membrane. (b) SEM image of a sample with as-grown suspended SWNTs crossing a gap and bridging metal electrodes. Scale bar: 2 μm . (c) SEM image of the sample shown in (b) after it was coated with silicon nitride by LPCVD. Scale bar: 2 μm .

^{a)}Also at: Department of Physics, Harvard University, Cambridge, MA 02138; electronic mail: golovchenko@physics.harvard.edu

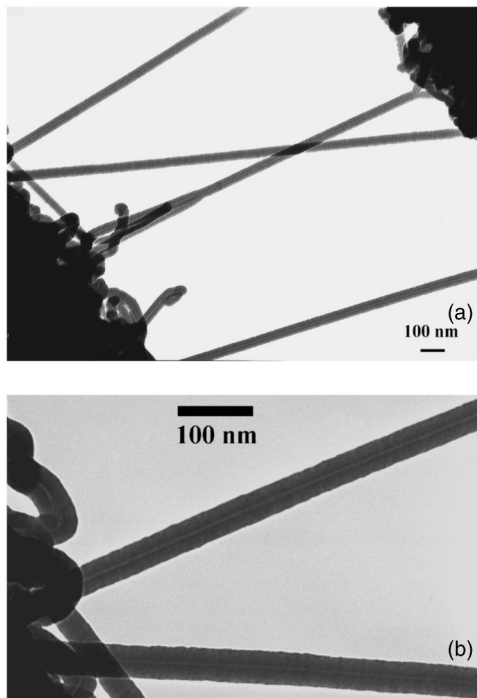


FIG. 2. (a) TEM image of suspended nanotubes after being coated with silicon nitride by LPCVD. Scale bar: 100 nm. (b) TEM image of two nanorods in the upper left of (a). Scale bar: 100 nm.

at a pressure ~ 1 Torr, the SEM image clearly shows that the suspended SWNTs are uniformly coated [Fig. 1(c)]. The diameters of the silicon nitride nanorods are about 200 nm, i.e., double the nominal growth on planar substrates, which is reasonable since on a suspended SWNT, silicon nitride will grow from all directions. Experimentally, we find that the thickness of the silicon nitride coating is controllable by the LPCVD reaction time.

To obtain more detailed structural information about the Si_3N_4 coating, we used TEM (60 kV) to study samples with thin Si_3N_4 layers. As shown by the TEM image in Fig. 2(a), nanotubes across a $1.5\text{-}\mu\text{m}$ -wide gap are coated with Si_3N_4 . For this sample, LPCVD was carried out at 720°C for 10 min, under conditions described previously. It is striking that all the nanotubes are coated uniformly and the diameters of the Si_3N_4 nanorods are similar. Also, the nanotubes buried in the center of the nitride are still visible in TEM, which demonstrates clearly that the nanotubes serve as the templates for the formation of silicon nitride nanorods. Figure 2(b) shows a higher magnification TEM image of the two nanorods in the upper left of Fig. 2(a). The diameters of the nanorods are ~ 45 nm, which is again about twice the value of the planar growth for this sample. The carbon nanotubes in the center core (brighter lines) are ~ 3 nm in diameter. The above-noted structural information shows clearly that LPCVD is able to coat SWNTs with uniform thickness in a controllable way. Moreover we will show that the coating does not damage the electrical contacts between the SWNTs and the electrodes, which is crucial for studying their electronic transport properties or making electronic devices.

To make a three-terminal device, we first coat a CVD grown suspended and electrically contacted nanotubes with thin Si_3N_4 layers (<30 nm) by LPCVD to protect the nanotubes. Then, we use the FIB to cut away all nanotubes but one metallic one which is left bridging the electrodes. Then

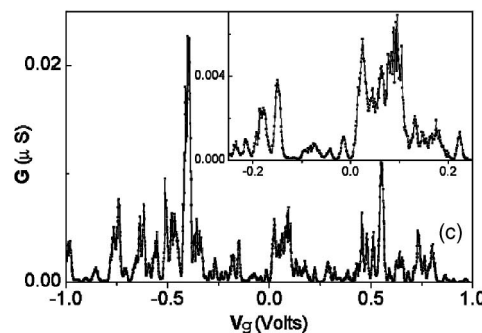
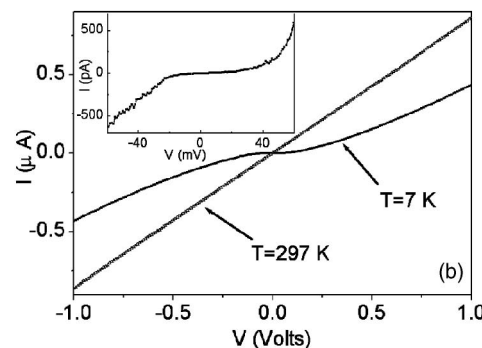
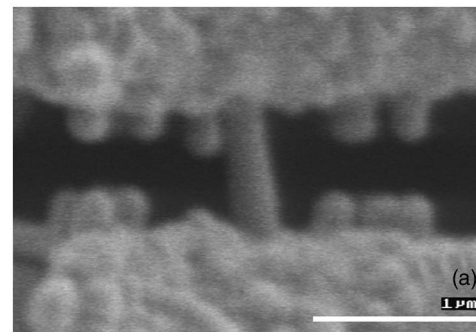


FIG. 3. (a) SEM image of one Si_3N_4 -coated nanotube bridging the source and drain electrodes covered by Si_3N_4 , before a top metal gate was patterned. Scale bar: $1\ \mu\text{m}$. (b) Source-drain I - V curves with gate voltage $V_g=0$ for the above-mentioned sample at room temperature (open triangles) and at a temperature $T=7$ K (closed squares). Inset: I - V curve near $V=0$ at $T=7$ K. (c) Conductance G vs gate voltage V_g recorded under a dc bias of 4 mV between source and drain at $T=7$ K. Inset: A zoom-in view of the conductance peaks near $V_g=0$.

another LPCVD process is carried out to insulate the open ends of nanotubes cut by the FIB, as well as coat the bridging nanotube with more Si_3N_4 . Figure 3(a) shows a SEM image of a particular sample with a single nanotube coated by Si_3N_4 , crossing a $1\text{-}\mu\text{m}$ -wide gap. The nitride nanorod is 250 nm in diameter, resulting from an initial 10 min LPCVD coating and a subsequent 40 min LPCVD coating after the cutting of other nanotubes. As seen clearly in the image, the remaining cut nanotubes are also coated with Si_3N_4 so that there is no open end which can be shorted to the gate electrodes evaporated in the next step of the process. Finally, we lithographically pattern a metal top gate (Au 25 nm/Cr 15 nm) in the gap area, which covers the coated nanotube as well as the ends of two coated electrodes (the source and the drain). The metal film is continuous from the surface of the Si_3N_4 nanorods to the insulating nitride layer on top of the source and the drain.

Figure 3(b) shows the source--drain I - V curves of the above mentioned sample at a gate voltage $V_g=0$ V. At room

temperature, the I - V curve is linear and virtually independent of the gate voltage V_g . At low temperatures, with high source-drain voltages, the I - V curves are near linear, and the conductance is on the same order of that at room temperature. However, at low source-drain voltages, the conductance is greatly suppressed by several orders of magnitudes and a gap clearly shows up [inset of Fig. 3(b)] by $T=7$ K. As described in the following, in our study of gate-voltage-dependent conductance, this is a consequence of the Coulomb blockade (CB) phenomena.^{14,15} The charging energy U is ~ 22 meV, which is half of the plateau in the I - V curve. As seen in Fig. 3(c), the linear conductance G versus gate voltage V_g exhibits Coulomb blockade oscillations. The inset shows a zoomed-in view of the CB peaks near $V_g=0$. These peaks have a spacing $\Delta V_g \sim 25$ mV. The height of different CB peaks is quite different, which can be attributed to the different coupling strength between the quantum levels inside the nanotube and the source (drain).¹⁴

Compared to reported results in the literature,^{15,16} there are two special features for our device made from a coaxially coated suspended nanotube. First, the charging energy U is several times larger than that reported for nanotubes lying on planar substrates.¹⁵ According to Ref. 15, the charging energy U is roughly ~ 5 meV for such a 1 - μm -long nanotube. Here the charging energy U is ~ 22 meV for a suspended nanotube 1 μm in length. Second, the conversion factor from gate voltage to electrostatic potential of the nanotube, i.e., $U/e\Delta V_g$, approaches unity, where ΔV_g is the period of CB peaks in gate voltage. These two features can be attributed to the unique geometry of the as-grown suspended nanotubes. The charging energy is $U=e^2/C$, where $C=C_l+C_r+C_g$, with $C_l(C_r)$ being the capacitance between the nanotube and the source (drain), and C_g the capacitance between the nanotube and the gate. Also, we have

$$\Delta V_g = \frac{C}{eC_g} \left(\Delta E + \frac{e^2}{C} \right),$$

where ΔE is the energy level spacing inside the one dimensional quantum dot (nanotube).¹⁴ For a 1 - μm -long nanotube,¹⁵ ΔE was estimated to be ~ 1 meV $\ll U \sim 22$ meV. Therefore, $e\Delta V_g \approx e^2/C_g$ and we have $e\Delta V_g/U \approx C/C_g = 1 + (C_l + C_r)/C_g$. In our case, $e\Delta V_g/U$ approaches unity, which means C_g dominates both C_l and C_r which is a consequence of the very small contact area between the nanotube and the source and drain electrodes¹³ making C_l and C_r small compared with C_g . Devices fabricated by the methods of Ref. 16 have large contact areas (thus large capacitances) between nanotubes and the junction electrodes yielding $e\Delta V_g/U \gg 1$ and negligible change of charging energy U even after the substrate material underneath the nanotube was etched away. However, in our case, since C_l and C_r are small, the charging energy U is much larger. Note that,

besides device geometry considerations, the observation of the large charging energy here can also be connected with the existence of defects in the nanotube so that only a short segment of it forms a quantum dot. However we have not observed the gate-tunable conductance of metallic nanotubes at room temperature as has been previously reported to characterize this situation.¹⁷

In summary, uniform coaxial coating of as-grown suspended single-walled carbon nanotubes with high-quality dielectric material silicon nitride has been successfully obtained by LPCVD. We anticipate that this approach, which is so highly compatible with more standard silicon device technology, will find applications in electromechanical,⁹ chemical sensors, and electronic devices fabricated from carbon nanotubes.^{7,8} Nanotube field effect transistors made in the described geometry, with suspended semiconducting nanotubes and coaxially coated dielectrics, should offer stable operation in a variety of environments with high transconductance. Future research should clearly focus on the limits to which thin functional gate dielectrics can be pushed for such devices.

The authors wish to acknowledge support for this research from DARPA, NSF, DOE, AFOSR, and Agilent Technologies.

¹S. Iijima, *Nature (London)* **354**, 56 (1991).

²Y. Zhang and H. Dai, *Appl. Phys. Lett.* **77**, 3015 (2000).

³A. Bezryadin, C. N. Lau, and M. Tinkham, *Nature (London)* **404**, 971 (2000).

⁴C. N. Lau, N. Markovic, M. Bockrath, A. Bezryadin, and M. Tinkham, *Phys. Rev. Lett.* **87**, 217003 (2001).

⁵J. Kong, N. R. Franklin, C. W. Zhou, M. G. Chapline, S. Peng, K. J. Cho, and H. J. Dai, *Science* **287**, 622 (2000).

⁶P. G. Collins, K. Bradley, M. Ishigami, and A. Zettl, *Science* **287**, 1801 (2000).

⁷S. J. Wind, J. Appenzeller, R. Martel, V. Derycke, and P. Avouris, *Appl. Phys. Lett.* **80**, 3817 (2002).

⁸A. Javey, H. Kim, M. Brink, Q. Wang, A. Ural, J. Guo, P. McIntyre, P. McEuen, M. Lundstrom, and H. Dai, *Nat. Mater.* **1**, 241 (2002).

⁹A. Husain, J. Hone, H. W.C. Postma, X. M.H. Huang, T. Drake, M. Barbic, A. Scherer, and M. L. Roukes, *Appl. Phys. Lett.* **83**, 1240 (2003).

¹⁰E. A. Whitsitt and A. R. Barron, *Nano Lett.* **3**, 775 (2003).

¹¹W. Han, and A. Zettl, *Nano Lett.* **3**, 681 (2003).

¹²T. Seeger, P. Redlich, N. Grobert, M. Terrones, D. R.M. Walton, H. W. Kroto, and M. Rühle, *Chem. Phys. Lett.* **339**, 41 (2001).

¹³H. B. Peng, T. G. Ristroph, G. M. Schurmann, G. M. King, J. Yoon, V. Narayanamurti, and J. A. Golovchenko, *Appl. Phys. Lett.* **83**, 4238 (2003).

¹⁴L. Kouwenhoven, C. M. Marcus, P. L. McEuen, S. Tarucha, R. M. Westervelt, and N. S. Wingreen, in *Mesoscopic Electron Transport*, edited by L. Kouwenhoven, G. Schön, and L. L. Sohn (Kluwer, Dordrecht, The Netherlands, 1997), pp. 105–214.

¹⁵J. Nygård, D. H. Cobden, M. Bockrath, P. L. McEuen, and P. E. Lindelof, *Appl. Phys. A: Mater. Sci. Process.* **69**, 297 (1999).

¹⁶J. Nygård, and D. H. Cobden, *Appl. Phys. Lett.* **79**, 4216 (2001).

¹⁷M. Bockrath, W. Liang, D. Bozovic, J. H. Hafner, C. M. Lieber, M. Tinkham, and H. Park, *Science* **291**, 283 (2001).